OBSERVATION STRATEGIES AND MEGACONSTELLATIONS IMPACT ON CURRENT LEO POPULATION

Giacomo Acciarini(1), Nicola Baresi(1), Christopher Bridges(1), Leonard Felicetti(2), Stephen Hobbs(2), and Atılım Güneş Baydin(3)

(1)*Surrey Space Center, University of Surrey, Guildford, GU2 7XH, United Kingdom, Email: {g.acciarini, n.baresi, c.p.bridges}@surrey.ac.uk*
(2)*School of Aerospace, Transport Systems and Manufacturing, Cranfield University, Cranfield, Bedford, MK43 0AL, United Kingdom, Email: {leonard.felicetti, s.e.hobb}@cranfield.ac.uk*
(3)*Dept. of Engineering Science & Dept. of Computer Science, University of Oxford, Parks Road, OX1 3PJ, Oxford, United Kingdom, Email: gunes@robots.ox.ac.uk*

ABSTRACT

The risk of collisions in Earth's orbit is growing markedly [19]. In January 2021, SpaceX and OneWeb released an operator-to-operator fact sheet that highlights the critical reliance on conjunction data messages (CDMs) and observations, demonstrating the need for a diverse sensing environment for orbital objects. Recently, the University of Oxford and the University of Surrey developed, in collaboration with Trillium Technologies and the European Space Operations Center, an open-source Python package for modeling the spacecraft collision avoidance process, called Kessler [2]. Such tools can be used for importing/exporting CDMs in their standard format, modeling the current low-Earth orbit (LEO) population and its short-term propagation from a given catalog file, as well as modeling the evolution of conjunction events based on the current population and observation scenarios, hence emulating the CDMs generation process of the Combined Space Operations Center (CSpOC) [1, 25]. The model also provides probabilistic programming and ML tools to predict future collision events and to perform Bayesian inference (i.e., optimal use of all available observations).

In the framework of a United Kingdom Space Agency-funded project, we analyze and study the impact of megaconstellations and observation models in the collision avoidance process. First, we monitor and report how the estimated collision risk and other quantities at the time of closest approach (e.g. miss distance, uncertainties, etc.) vary, according to different observation models, which emulate different radar observation accuracy. Then, we analyze the impact of future megaconstellations on the number of warnings generated from the increase in the number of conjunctions leading to an increased burden on space operators. FCC licenses were used to identify credible megaconstellation sources to understand how a potential consistent increase in active satellites will impact LEO situational safety. We finally present how our simulations help understand the impact of these future megaconstellations on the current population, and how we can devise better ground observation strategies to quantify future observation needs and reduce the burden on operators.

Keywords: Megaconstellations; Space Debris; Spacecraft Collision Avoidance; Probabilistic Programming.

1. INTRODUCTION

The risk of collision in Earth's orbit is growing steadily. The advent of the New Space era and the launch of megaconstellations have accelerated this process [7]. Several studies have warned about the increased collision risk among objects, due to the predicted growth of the space sector [22, 32]. Currently, the US Strategic Command (USSTRATCOM) constantly tracks resident space objects via a global Space Surveillance Network (SSN) and updates a public catalog of two-line element (TLE) data. At the same time, the Combined Space Operations Center (CSpOC), which is a joint military organization responsible for the surveillance and tracking of man-made objects in Earth's orbit, constantly detects and identifies potential collisions between satellites and other objects in space. Once this is done, if a potential collision is detected, Conjunction Data Messages (CDMs) are issued to the owner/operators of those objects, to warn them of the potential collision. These messages contain information about the time and location of the potential collision and the relative velocity of the objects. Moreover, since CSpOC uses a network of ground-based radar and optical instruments to track objects and propagates this information at future times with an orbital propagator, they also have information on the dynamical models used for propagation and on the propagated uncertainties at the time of closest approach.

Albeit the thousands of objects in orbit, high-risk satellites conjunctions are very rare and it is difficult to ob-

Proc. 2nd NEO and Debris Detection Conference, Darmstadt, Germany, 24-26 January 2023, published by the ESA Space Safety Programme Office
Ed. T. Flohrer, R. Moissl, F. Schmitz (http://conference.sdo.esoc.esa.int, February 2023)

tain a high sample of data from the CDMs, especially because there is currently no open-source database that contains all the produced CDMs, and each operator can only access those pertaining to its operated objects. For this reason, we have developed Kessler: an open-source package for satellite conjunction analysis. The software, not only allows one to parse, analyze, and plot CDMs in their original format, but it also has a simulator that can emulate the entire CDM generation process. In this way, we can pass a certain LEO population to the software, and study what is the number of collision warnings that would be generated, and their characteristics. The simulator is a complete "white" box, and the user can inspect every variable involved in the conjunction. Moreover, it is also a probabilistic simulator, which means that one can combine the simulator with observational data (e.g. tracking data, TLEs, CDMs, or else) and use Bayesian inference to quantify and update the uncertainties of model parameters given the available observations (i.e., posterior distribution).

In this work, we show how to use our probabilistic model for two case studies. First, we study the impact of planned megaconstellations in the current LEO environment. Then, we investigate the influence of observation accuracies in satellite conjunction analysis. The paper is organized as follows: Section 2 introduces some previous work concerning spacecraft collision avoidance and megaconstellations impact. In Section 3 we outline the characteristics of Kessler software, by first discussing its functionalities, and by then describing the probabilistic model of conjunctions. Then, in Section 4 we discuss the two conducted case studies: the first one about observation accuracies, the second one about megaconstellation impact. Finally, in Section 5, we discuss the conclusions and implications of our work.

2. BACKGROUND

2.1. Spacecraft Collision Avoidance

Nowadays, although active debris removal is progressing fast, with the first missions being launched, it is, however, not fully implemented yet so that it can remediate collisions between space objects. Instead, to reduce the collision risk, operators still rely on CSpOC data (derived from constant monitoring and prediction of space objects' trajectories), and collision avoidance maneuvers (if one of the two objects can be maneuvered). While each space agency has its own software and strategy to deal with satellite collision avoidance, there are, however, common denominators among all agencies. First of all, almost all the agencies interact with CSpOC, which is the main source of CDM data worldwide. Secondly, they all integrate this external information with their own tracking (e.g. using GPS) and orbital propagation (e.g. high fidelity orbital propagators internally maintained by the agency) tools. Thirdly, they all propagate the objects' position and uncertainties until the time of closest approach, and they assess the probability of collision resulting from the event. If that probability exceeds a defined threshold, maneuvers might be performed to reduce the collision risk. For each space agency, there might be differences in the techniques used to propagate the objects and their uncertainties, the algorithms implemented to assess the collision risk, the decision to perform a maneuver or not, and how to perform it. Several previous works have discussed in great detail the differences in the collision avoidance strategies between space agencies (i.e., CNES, DLR, ESA, NASA, JAXA, CSA) [29, 21, 11, 3, 23, 18, 15, 10].

2.2. Megaconstellations

Several private companies are currently launching or planning to launch satellite megaconstellations. These are groups of satellites (typically in the order of hundreds or thousands) launched to provide worldwide internet coverage or other services in space. Some examples include SpaceX Starlink, OneWeb, Amazon Kuiper, Guowang, and many others. As of September 2020 (when less than 1,000 Starlink satellites were launched), Starlink already amounted to 90% daily CDMs produced by the 18th Space Control Squadron, which corresponded to 180,000 daily messages [14]. As of November 2022, there are more than 3,000 active Starlink satellites in orbit[1], which is more than 50% of the active satellite population and about 10% of the overall population of space objects above 10 cm in LEO. With the recent trends, this number is expected to increase: soon, megaconstellation satellites might reach or even pass the total number of active and inactive satellites. This raised concerns across different communities. In particular, three are the main discussed aspects regarding megaconstellations:

1. the increase in the number of satellite conjunctions, especially high-risk ones, which eventually leads to more satellite collisions. Such collisions would increase the number of space debris and, consequently, the possibility of triggering a Kessler syndrome (that is, a cascade of collisions that would make space hardly accessible) [16]. Several studies have investigated the impact of megaconstellations in the current LEO environment, in terms of collision risk [27, 28, 30, 8, 35]. Most of these studies, when they are not based on observational data (i.e., GPS data or CDMs), they are either long-term simulations of the space population (i.e., for 100 years or more) using debris flux assumptions (e.g. employing molecular gas dynamics assumptions), or they are limited to qualitative analysis [31, 26, 24]. In this work, our objective is to show how Kessler software can be used to analyze and quantify the short-term impact of megaconstellations in terms of the burden on space operators and collisions;

[1] `https://www.space.com/spacex-starlink-satellites.html`

2. another concern is related to the impact of these satellites on ground-based astronomical observations. Indeed, this high number of satellites in LEO can generate light pollution, which hinders astronomers' capability of observing the sky [13, 20];

3. finally, these megaconstellations can also impact communication and navigation systems, due to interferences [9].

While the challenges of megaconstellations are apparent, there is currently no open-source tool that allows studying the impact of megaconstellations on a given space environment, by simulating the short-term collision risk between satellites and by producing statistical reports (e.g. detailing the expected increase of high-risk events, the satellites that are most in danger, etc.). Such a tool could be very powerful in quantitatively assessing megaconstellation impact and could also be used in the design of these constellations. This could, for instance, aid in trying to alleviate the burden on operators, the number of maneuvers, and the risk of collision, when designing a constellation. One of the objectives of this paper is to show how Kessler software can be used to bridge this gap.

3. COLLISION AVOIDANCE ANALYSIS WITH KESSLER SOFTWARE

3.1. Functionalities

Kessler[2][3] is a Python package for simulation-based inference and satellite conjunction analysis. It was initially created in 2020 by some of the authors in collaboration with the ESA European Space Operations Center during an 8-week research sprint enabled by Frontier Development Laboratory[4]. The main functionalities of the tool can be divided into three categories:

1. CDM parsing and analysis: this concerns the set of utilities offered to import, export, plot, group, and analyze conjunction data messages in their original format. This tool can be useful for those who have a set of real or synthetically generated CDMs and want to investigate their characteristics or export them into different formats (e.g. csv). Each set of CDMs belonging to a conjunction event is represented with a Python class, whose attributes and methods allow users to intuitively and quickly output and/or visualize the needed information of the conjunction event.

2. Deep learning module: this refers to the set of functionalities to train, save and load long-short term memory (LSTM) networks to be used on a given set of CDM data. With a few lines of code, Kessler enables the user to load an LSTM and train it on a dataset of CDMs, by just specifying the neural network hyperparameters and the features to be used for training.

3. Probabilistic programming module: this provides a simulator that can generate conjunction events and their corresponding CDMs. This module offers simulation functionalities to generate many synthetic conjunction events, as well as the probabilistic inference framework to update our beliefs about the probability density functions of latent variables, given our current knowledge, as new observations become available. Due to the central role of this module in the presented experiments, we devote the next section to its description.

3.2. Probabilistic Program for Satellite Conjunctions

One of the key modules in the Kessler software is its probabilistic programming module [1, 2]: this term refers to a paradigm that allows defining a simulator (i.e., generative model) that can be used for either generating data (i.e., through forward run of the simulator) or for performing Bayesian inference on latent variables conditioned on observed data (i.e., solving the inverse problem) [34, 6]. Before delving into the simulator properties, it is first important to clarify three fundamental ingredients of any Bayesian model. Given a vector of latent parameters (i.e., the inputs $\mathbf{x}$) and a set of sample data (i.e., the outputs $\mathbf{y}$), which arise as observations, we identify the following three probability density functions:

1. prior distribution $p(\mathbf{x})$: this is the probability density function (pdf) that models the initial belief about the latent parameters of the model, before taking into account observations. In the context of satellite conjunction analysis, this it describes the initial state of the target and chaser objects;

2. likelihood $p(\mathbf{y}|\mathbf{x})$: this represents the probability of the observations given the model's latent parameters. For instance, it could be the probability of observing a certain position and velocity of the satellites, given their ground truth position and velocity, and the measurement noise;

3. posterior distribution $p(\mathbf{x}|\mathbf{y})$: this is the updated belief about the latent variables of the model, after taking into account the new observations/data. The posterior describes how we quantify the chances of the true value of the latent parameters belonging in different parts of the parameter space (i.e., Ω), depending on the observed data: this process is known as Bayesian inference, and it involves the use of Bayes' theorem to find the posterior distribution:

$$p(\mathbf{x}|\mathbf{y}) = \frac{p(\mathbf{y}|\mathbf{x})p(\mathbf{x})}{\int_{\Omega} p(\mathbf{y}|\mathbf{x})p(\mathbf{x})}$$

[2] https://kessler.readthedocs.io/en/latest

[3] https://github.com/kesslerlib/kessler

[4] https://fdleurope.org/about-fdl

Typically, the complexity of the problem and the size of the latent space do not allow finding the posterior distribution in a closed form. For this reason, sampling and approximation techniques are usually needed [5].

The simulator requires the definition of the above three probability density functions. Once these are specified, the model can either run forward, in which case the joint probability density function of the model parameters and simulated observations (i.e., $p(\mathbf{x}, \mathbf{y})$) can be extracted. Or it can also run backward, via Bayesian inference: if external observations of the real process (i.e., CDMs or tracking data or else) are available, then Bayesian inference (e.g. through Markov chain Monte Carlo or importance sampling or other techniques) can be performed and the model parameters and their uncertainty distribution can be updated and calibrated to real observations.

But how do we exactly construct the simulator and leverage the probabilistic programming framework, in the context of satellite conjunction analysis? The first step is to define the generative model, this is a simulator that emulates the real process through which CDMs are generated, from the simulation of space objects in orbit to the detection of conjunction, the forecast of the closest approach, and the associated collision probability, as well as the observation schedule and the CDMs generated for each conjunction event. Usually, a conjunction is detected whenever the predicted distance between any pair of objects (i.e., target and chaser) in space goes below a certain conjunction threshold. If that is the case, a time of closest approach (TCA) is identified, and CDMs that contain information on the propagated covariance and state at TCA, as well as other information involving the propagation, are released, roughly every 8 hours (if new observations about either object are made available). A diagram summarizing the simulator and the forward and inference processes is shown in Figure 1. In summary, its steps can be condensed as follows:

1. target and chaser trajectories are generated for a 7 days period after sampling prior distributions;
2. if the two objects reach a minimum distance below a certain threshold (i.e., the conjunction threshold), which defines the distance at which a conjunction event is considered potentially dangerous and is therefore observed, then the CDM generation process is triggered;
3. for generating the CDMs, the TCA (and the corresponding distance) are identified, and the objects are observed according to a pre-defined observation strategy (e.g., in terms of measurement noise and frequency of the observations);
4. for each observation, each object and its uncertainties are propagated up to the TCA, where the probability of collision is computed and recorded, together with all the other CDM information (e.g. the covariances of both objects at TCA, their relative distance and speed, etc.);
5. once all the CDMs are generated, the process is terminated and an object containing all the CDMs, together with the latent variables, the sample data, and any other variable involved in the process, is returned;

In the above, three aspects are particularly crucial and worth further discussion: how to generate observations of the object and assign them a certain measurement noise, how to propagate the uncertainties at TCA, and how to compute the probability of collision.

Observations: at discrete times (depending on the observation strategy) observations of the target and chaser objects are taken. Currently, we model these as TLEs. Roughly, every 8 hours, if the object has to be observed, a TLE and its associated measurement noise are generated corresponding to that object. For doing this, the user has to only specify the measurement noise in terms of the covariance matrix in the RTN-frame. In this way, we model plausible observations (and associated uncertainties) made on the target and/or chaser objects. The uncertainty in the observations is induced by measurement errors and depends on the state of the object when it is observed (i.e., depending on the state of the object, an object observed with the same instrument generates different uncertainties). Therefore, the observation uncertainty represents the likelihood function: $p(\mathbf{y}|\mathbf{x})$.

Uncertainty propagation: for this, a sample-based Monte Carlo approach is used. Many samples are generated at the observation times using the observed mean and covariance, and the objects are then propagated at TCA. Then, at TCA, the mean and covariance matrix are extracted and stored within the CDMs. This is repeated for each observation time.

Probability of collision: once the probability density functions of both objects at TCA are found, we have to assess the probability of collision. This involves solving the following integral:

$$P_c = \int_{\Omega_r} p_t(\mathbf{r}_t) p_c(\mathbf{r}_c) I(|\mathbf{r}_t - \mathbf{r}_c|), \tag{1}$$

where p_t and p_c are the probability density functions of the positions of target and chaser at TCA, and I is the indicator function that is 1 if the two objects are within a certain collision distance, which is known as hard body radius, and 0 otherwise:

$$I = \begin{cases} 1 & \text{if } |\mathbf{r}_t - \mathbf{r}_c| < \bar{r} \\ 0 & \text{otherwise} \end{cases},$$

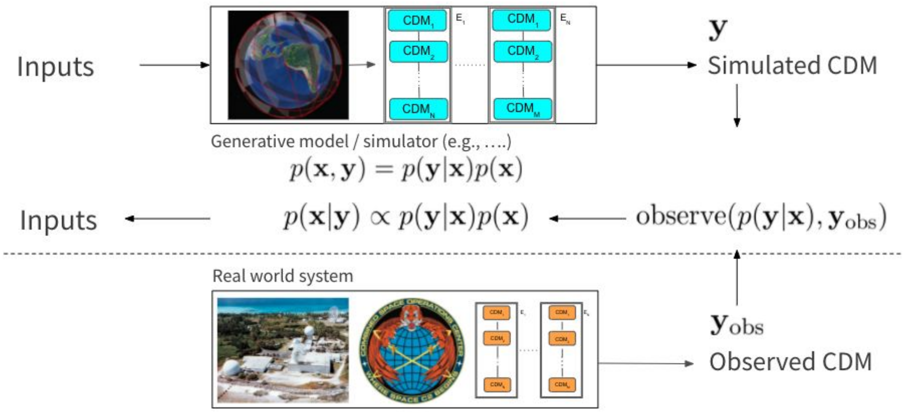

Figure 1: .

where $\bar{r}$ is the hard body radius. The integral expressed in Equation (1) cannot be solved in a closed form and requires an approximation. In our model, we use a sampling-based technique. Both probability density functions are sampled at TCA, and the distance between each pair of samples is computed. Then the number of the pairs below the hard body distance is divided by the total number of samples, which returns an estimation of the collision probability: this method would return the exact probability of collision for infinite samples. In general, the higher the samples, the better the ability to detect low probabilities.

4. EXPERIMENTS

We divide the experiments into two categories: megaconstellations impact experiments and observations accuracy experiments. In the former, we simulate the presence of 5 different megaconstellations (i.e., SpaceX Starlink, OneWeb, Amazon Kuiper, GuoWang, and SatRevolution) and we quantify their impact in the satellite conjunction analysis process, by evaluating the high-risk events, the number of increased CDMs and the number of increased conjunctions. Then, we perform experiments investigating the importance of observation accuracy in accurately describing conjunctions between satellites and their associated risk. For this purpose, we run the same conjunctions with 5 different observations accuracies (for both chaser and target), and we quantify the impacts on satellite conjunctions assessment. All the experiments are run by setting a hard body radius distance of 70 meters, and by computing the collision probability using 10 billion pairs, and ignoring any P_c values lower than 10^{-8}. The experiments have the objective to show two use cases in which Kessler effectively helps in assessing conjunctions between satellites. In all cases, the baseline LEO population used in all experiments is derived as of March 2022 from public TLE files, downloaded from Space-Track[5].

[5]https://www.space-track.org/

4.1. Megaconstellations Impact

We simulate 5 different scenarios where we add 5 megaconstellations to the LEO population, whose parameters are derived from the files published by the Federal Communications Commission (FCC). The following constellations have been simulated:

1. SpaceX Starlink[6] Generation 1 fleet of 4,408 satellites. This comprises 5 groups of satellites, with altitudes: 550 km, 570 km, 560 km, 540 km, 560 km; inclinations: 53°, 70°, 97.6°, 53.2°, 97.6°; number of planes: 72, 36, 6, 72, 4; satellites per plane: 22, 20, 58, 22, 43.

2. OneWeb[7] (from its 2020 filings) fleet of 48,564 satellites. This comprises 4 groups of satellites, all with altitudes of 1,200 km; inclinations: 87.9°, 87.9°, 40°, 55°; number of planes: 18, 36, 32, 32; satellites per plane: 720, 1764, 23,040, 23,040.

3. Amazon Kuiper[8] fleet of 3,452 satellites. This comprises 3 groups of satellites, with altitudes: 590 km, 610 km, 630 km; inclinations: 33°, 33°, 33°; number of planes: 28, 42, 34; satellites per plane: 28, 36, 34.

4. Guo Wang[9,10] (both GW-A59 and GW-2) fleet of 12,992 satellites. This comprises a total of 7 groups of satellites, with altitudes: 590 km, 600 km, 508 km, 1,145 km, 1,145 km, 1,145 km, 1,145 km; number of planes: 16, 40, 60, 48, 48, 48, 48; satellites per plane: 30, 50, 60, 36, 36, 36.

[6]https://docs.fcc.gov/public/attachments/FCC-22-91A1.pdf

[7]https://fcc.report/IBFS/SAT-MPL-20200526-00062/2379706.pdf

[8]https://docs.fcc.gov/public/attachments/FCC-20-102A1.pdf

[9]https://www.itu.int/ITU-R/space/asreceived/Publication/DisplayPublication/23708

[10]https://www.itu.int/ITU-R/space/asreceived/Publication/DisplayPublication/23706

5. SatRevolution[11] fleet of 1,024 satellites. This comprises 2 groups of satellites, both with altitudes around 520 km; inclinations: 97.5°, 60°; number of planes: 1, 1; satellites per plane: 512, 512.

For all simulated scenarios, we exclude possible conjunctions between objects belonging to the same megaconstellation. Moreover, for the case of Starlink and OneWeb, due to the fact that some of them have already been launched and are operative as of March 2022, we simulate both the case in which they are fully deployed, and also when none of them is in orbit, in order to quantify their influence on satellites' conjunctions. In Figure 2, we display the distribution of the semi-major axis and inclinations of objects in LEO for the cases in which the constellations are fully deployed, as well as their values as of March 2022 (referred to as *Base* in the figure). As we would expect, the probability density functions tend to peak for the inclination and semi-major axis values at which these constellations are deployed: this is accentuated for OneWeb since it is the constellation with most objects.

We ran these different LEO populations in Kessler until 1,000 conjunctions below 5 km were found. In practice, this means that the program keeps sampling the prior until that number of conjunctions is found. Each conjunction generates a series of CDMs, which can go from 1 (the event is only detected 8 hours before TCA) to 20 (the event is detected 7 days before TCA). In total, we synthetically generated more than 70,000 CDMs, which are then used, together with the ground truth information of the target and chaser trajectories and characteristics, to inspect the conjunction parameters. In Figure 3 and 4, we show different groups for the probability of collision and the ground truth distance at TCA, respectively, as a function of their occurrences in the simulated 1,000 conjunctions (e.g. 30% implies that 300 conjunctions were found with those characteristics). The first figure does not contain the events that have resulted in probabilities below 10^{-8}, which amounted to roughly 60% of all conjunctions, for all simulations. As we can observe, more than 90% of the conjunction events display probabilities of collision below 10^{-4}, while no events were found with probabilities above 10^{-2}. This shows how rare these events can be (considering that we are already filtering for only cases below 5 km). In particular, the second plot can be used to understand how frequent a given conjunction event is as a function of the distance at TCA. By fitting the d_{TCA} distribution, we can gain useful information about the portion of events that we expect to have below a certain minimum TCA distance. We, therefore, fitted an exponential function to the given data. In particular, we first removed all the events below 1,200 m (since we could only find very few from the generated data, and we deemed them not representative of the behavior of the distance). Then, we fitted an exponential function of the form:

$$y = ae^{bx} + c,$$

[11] https://www.itu.int/ITU-R/space/asreceived/Publication/DisplayPublication/28529

where a,b,c are the coefficients to fit, while x is the d_{TCA} and y is the occurrence. In Figure 5, we show the resulting exponential fit together with the data. This can be used to inform operators and agencies on the expected number of CDMs for a given distance threshold. For instance, if the 18th Space Control Squadron manages (e.g. thanks to improvements in the observation sensors) to reduce the threshold at which a CDM is generated to about 1.2 km, then our model predicts that only about 0.01% of the currently released CDMs would be generated. This would greatly alleviate the burden on space operators.

As we can observe from Figure 3 and 4, there seem to be no significant differences in terms of probability of collision and minimum distance distributions between the different megaconstellation cases, and also between those cases and the ones without any constellation. This seems to suggest that none of these constellations displays a particular orbital geometry that results in higher risk events, compared to the current scenario. Nevertheless, when looking at the increased frequency of these conjunction events due to the presence of megaconstellations, the situation changes considerably. By looking at the objects involved in the conjunction events, we can derive how many of the simulated conjunctions were due to the megaconstellations: these are about 70% for Starlink, 96% for OneWeb, 38% for Kuiper, 55% for Guo Wang and 26% for SatRevolution. This means that when these constellations are deployed, events below 5 km are produced at a much faster pace. Starlink would cause a 3.3× increase in number of conjunctions below 5 km, while OneWeb an astonishing 250× increase, Kuiper a 1.6× increase, Guo Wang a 2.2× increase, and SatRevolution a 1.35× increase.

Finally, the generated CDMs can also be used to understand what are the most dangerous objects in the studied scenarios. Excluding the constellation objects (which are always the most frequent), the most found dangerous objects for the studied scenarios and their corresponding frequency of occurrence are shown in Table 1. As we can observe, the debris generated by either previous collisions (e.g. COSMOS 2251) or ASAT tests (e.g. COSMOS 1408, FENGYUN 1C) are those that pose the higher collision risk to the current satellites. This corroborates the importance to put a stop to anti-satellite tests in space, and to have laws that regulate the use and safeguarding of space. Furthermore, we can also see that the case with OneWeb fully deployed is the only one in which the most encountered object in the conjunctions is SL-14 and not COSMOS 1408. The reason is attributed to the fact that nearly 96% of the conjunctions for the OneWeb case are due to OneWeb satellites, which happen to fly at a much higher altitude than the other megaconstellation (i.e., 1,200 km altitude) and are, therefore, more subject to the risks posed by the higher altitude SL-14 debris than the COSMOS 1408 ones.

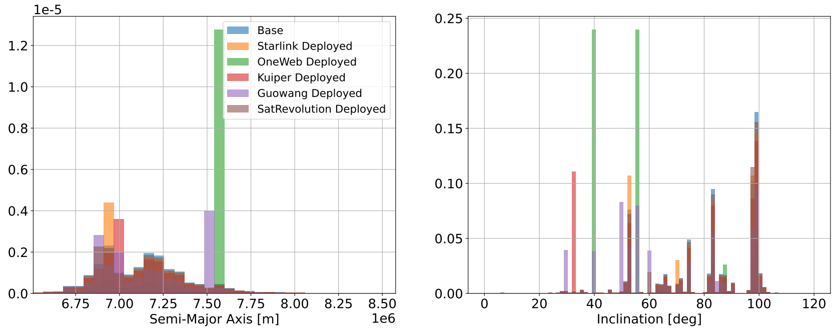

Figure 2: Semi-major axis and inclination for the simulated experiments.

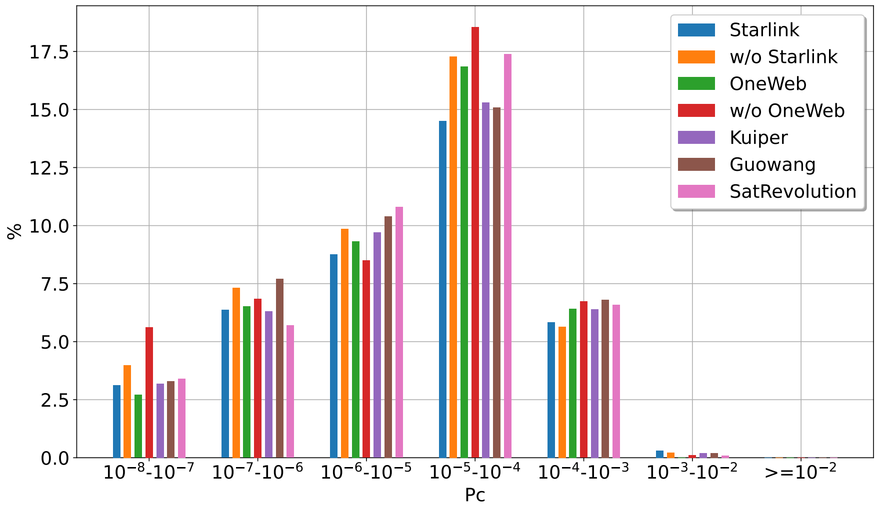

Figure 3: *x-axis*: the probabilities of collision grouped in bins (probabilities below 10^{-8} are not displayed; *y-axis*: frequency of appearance of those distances, w.r.t. all the conjunctions simulated for each case.

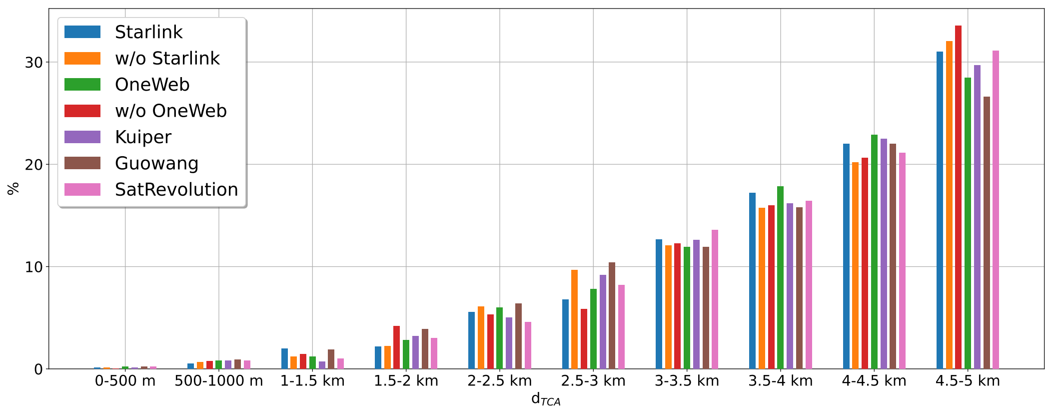

Figure 4: *x-axis*: the distance at TCA between chaser and target grouped in bins; *y-axis*: frequency of appearance of those distances, w.r.t. all the conjunctions simulated for each case.

Table 1: A table illustrating the objects that are more involved in collisions on the performed experiments: megaconstellations are excluded and treated separately. Each cell contains the name of the satellite name and the percentage at which that satellite appeared in the simulated conjunctions.

Experiments	Object 1	Object 2	Object 3	Object 4
Starlink	COSMOS 1408 DEB, 14.75%	FENGYUN 1C DEB, 9.53%	COSMOS 2251 DEB, 5.32%	TBA - TO BE ASSIGNED, 4.66%
w/o Starlink	COSMOS 1408 DEB, 10.70%	FENGYUN 1C DEB, 4.96%	COSMOS 2251 DEB, 3.03%	TBA - TO BE ASSIGNED, 2.51%
OneWeb	SL-14 DEB, 18.96%	FENGYUN 1C DEB, 5.57%	TBA - TO BE ASSIGNED, 5.27%	DELTA 1 DEB, 3.41%
w/o OneWeb	COSMOS 1408 DEB, 12.75%	FENGYUN 1C DEB, 7.84%	TBA - TO BE ASSIGNED, 3.75%	COSMOS 2251 DEB, 3.59%
Kuiper	COSMOS 1408 DEB, 9.95%	FENGYUN 1C DEB, 4.85%	RESURS O1 DEB, 4.15%	COSMOS 2251 DEB, 3.75%
Guowang	COSMOS 1408 DEB, 9.65%	FENGYUN 1C DEB, 3.75%	TBA - TO BE ASSIGNED, 2.50%	COSMOS 2251 DEB, 2.10%
SatRevolution	COSMOS 1408 DEB, 14.55%	FENGYUN 1C DEB, 5.80%	COSMOS 2251 DEB, 3.05%	TBA - TO BE ASSIGNED, 2.00%

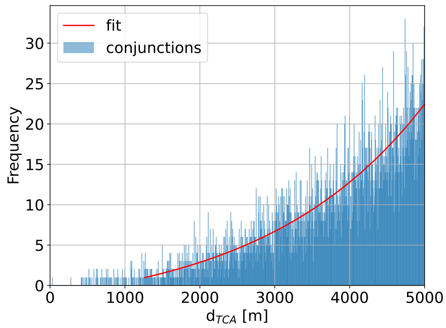

Figure 5: Histogram of the TCA distance for all the experiments, together with its exponential fit, shown in red.

4.2. Observations Accuracy

In the second case study, we investigated how different observation strategies can affect CDMs and the collision avoidance process in general. In particular, we modeled the measurement noise using 5 different RTN-covariance matrices for chaser and target. For all experiments, we assumed a diagonal RTN-covariance matrix for the measurement uncertainty. The strategies were defined as follows [12]:

1. Strategy 1: the target is observed extremely accurately, the diagonal terms of the covariance matrix are $Cov_{RTN,t}$=[0.82 m, 1.5 m, 0.5 m, 0.0001 m/s, 0.0001 m/s, 0.0001 m/s]^2, while for the chaser one: $Cov_{RTN,c}$=[120/3 m, 600/3 m, 120/3 m, 0.0001 m/s, 0.0001 m/s, 0.0001 m/s]^2;

2. Strategy 2: in this case, the target covariance was chosen as $Cov_{RTN,t}$=[120/3 m, 600/3 m, 120/3 m, 0.0001 m/s, 0.0001 m/s, 0.0001 m/s]^2, and $Cov_{RTN,c}$=[120 m, 600 m, 120 m, 0.0001 m/s, 0.0001 m/s, 0.0001 m/s]^2;

3. Strategy 3: in this case, the target covariance is the same as Strategy 2, and the chaser one is $Cov_{RTN,c}$=[240 m, 1,200 m, 240 m, 0.0001 m/s, 0.0001 m/s, 0.0001 m/s]^2;

4. Strategy 4: also in this case, the target covariance is the same as Strategy 2, while the chaser one is $Cov_{RTN,c}$=[480 m, 2,400 m, 480 m, 0.0001 m/s, 0.0001 m/s, 0.0001 m/s]^2

5. Strategy 5: this case also has the same target covariance as Strategy 2, but the chaser one is $Cov_{RTN,c}$=[960 m, 4,800 m, 960 m, 0.0001 m/s, 0.0001 m/s, 0.0001 m/s]^2

Using these strategies, we simulate about 30 conjunction events below 5 km with 20 CDMs each and test each of the strategies on the same conjunctions. Each conjunction is observed for a period of 7 days: the first CDM (i.e. CDM 1) is received about 7 days before the TCA, while the last (i.e., CDM 20) is received about 8 hours before, and they are updated every 8 hours. Our objective is to assess how the state and the covariance matrix at TCA are affected by different observation accuracies. In Figure 6, we show how the covariance matrices diagonal terms at TCA vary for one of the simulated events, as a function of the received CDMs (in general, the covariances at TCA become non-diagonal, but we here only show the diagonal terms to reduce the number of images). The closer the CDM is to TCA, the lower the covariance values tend to be, due to the fact that the initial covariance is propagated for shorter time horizons. Moreover, we observe that some of the covariances of the target overlap: the reason is due to the fact that the same target covariance is used for 4 experiments. To better appreciate the fact that the covariance volume tends to shrink as the CDMs approach TCA, we compute the determinant of the covariance matrices at TCA: this can be seen as a generalized variance, which measures the dispersion around the mean [33]. We average these values across all simulated conjunction events, and we display the results as a function of the CDMs in Figure 7. As one would expect, the more the observation strategy is accurate, the lower the determinant is. Furthermore, it is also confirmed that the closer we get to the TCA, the lower the determinant becomes.

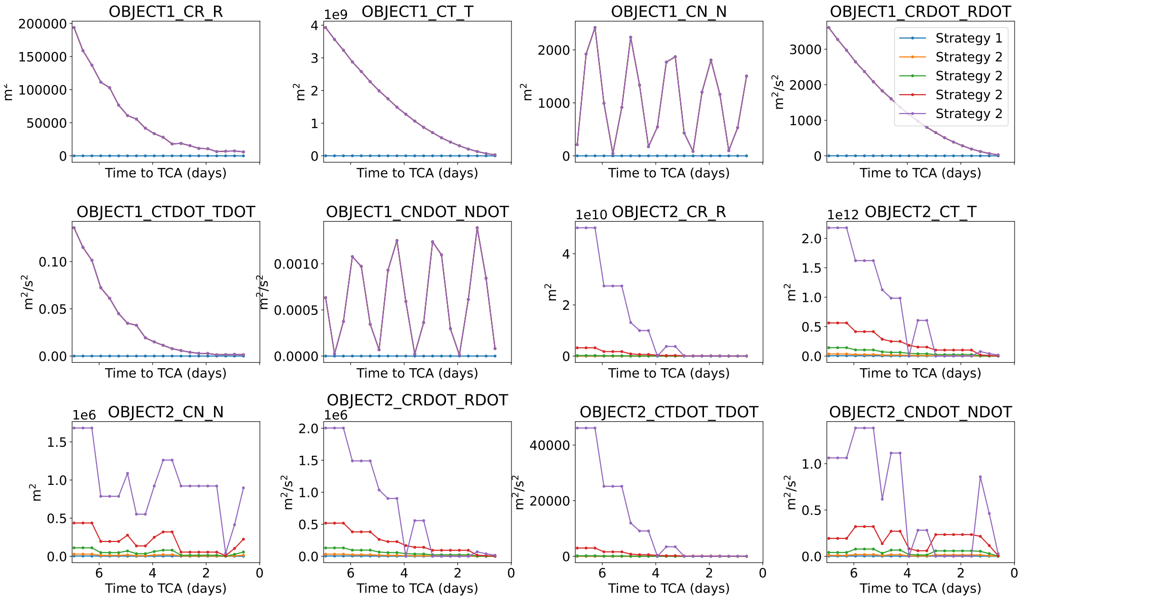

Figure 6: Diagonal terms of the covariance matrix at TCA as a function of the received CDMs (from the first received 7 days earlier, to the 20th one, 8 hours before TCA) for the five different tested observation strategies.

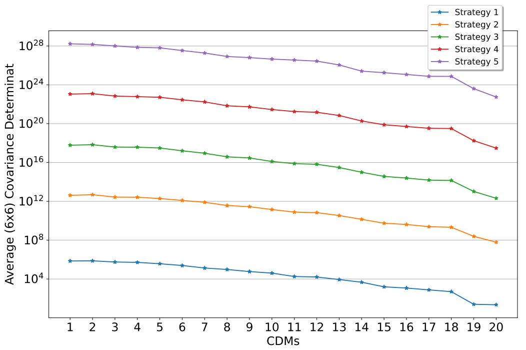

Figure 7: Determinant of the covariance matrices at TCA as a function of the received CDMs for the five different observation strategies.

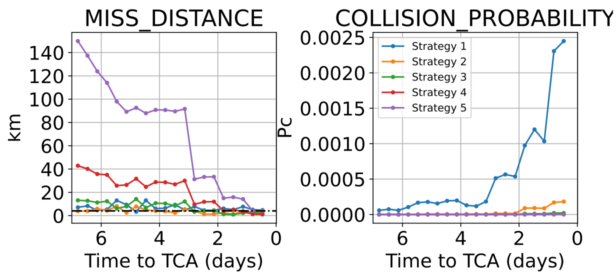

Figure 8: Estimated miss distance and probability of collision as a function of time to TCA, using 5 different observation strategies, for one of the simulated events. In the miss distance figure, we show as a black dotted line the ground truth distance between the chaser and target at TCA.

What are the implications of these covariance values on the estimated distance and risk of collision at TCA? In Figure 8, we show how the estimated miss distance and probability of collision vary as a function of the time to TCA, for the five different observation strategies. It is clear that the least accurate strategies can lead to big errors in the estimation of the miss distance between the two objects, while more accurate ones (e.g. Strategy 1 and 2) manage quite successfully to estimate the true miss distance, even several days before the TCA (as it can be confirmed by comparing their values to the black dotted line, which represents the ground truth distance at TCA). In order to assess how the estimation of the miss distances changes as a function of the different observation strategies, we compute the mean absolute percentage error between the estimated miss distance, and the ground truth one. The results are displayed in Figure 9, as a function of the received CDMs. Again, it is possible to confirm that the closer we are to TCA, the lower the error in the evaluation of the miss distance. However, the difference can be considerable, depending on the accuracy of the observations. As it can be observed, Strategy one reaches an error of less than 10% in MAPE for the last CDM, while the other strategies are all above 90%. This shows how crucial measurement accuracy is in the collision avoidance process, and how improvements in this area can bring massive advantages in terms of reduction of the collision risk.

When looking at the probability of collision plot on the right side of Figure 8, we also observe how large covariances lead to the well know probability dilution problem [4, 17]. That is when the covariances of both objects are extremely large (e.g. big measurement errors) then

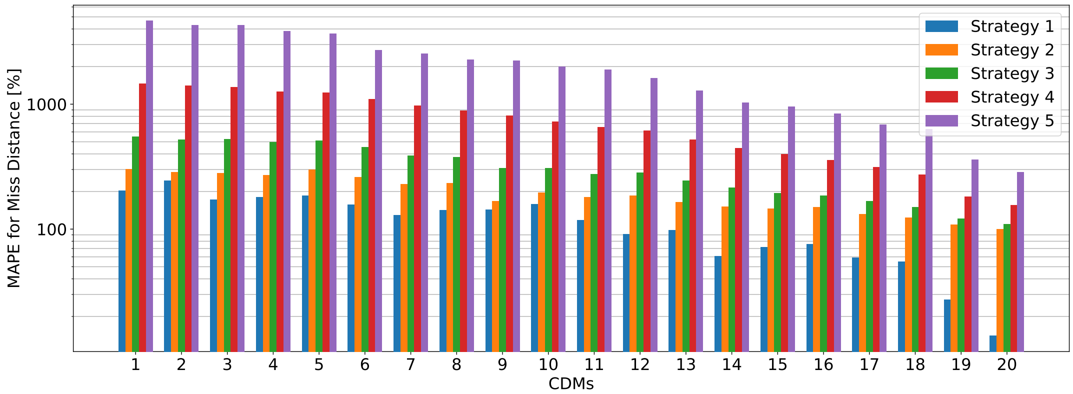

Figure 9: Mean absolute percentage error between the estimated miss distances and the ground truth distance at TCA, as a function of the received CDMs, with the first CDM received about 7 days before TCA, and the last about 8 hours before (and regularly space at about 8 hours intervals).

the probability of having the two objects at a distance below the hard body radius tends to zero, which causes their probability of collision to go to zero: however, this is only driven by the fact that the orbits of the two objects are poorly known. There is therefore the paradox in which little certainty on the objects' states leads to a vanishing probability of collision. This can be clearly seen on the right side of figure 8. The situation, in the displayed case, is even more worrying because the event, for the most accurate observation scenario (strategy 1) shows a high probability of collision (more than 1 out of 1,000) and with an increasing behavior as a function of time to TCA: such events are typically those who typically require an operational maneuver, whenever possible.

5. CONCLUSIONS

In this paper, we discussed the use of Kessler software, an open-source Python package for collision avoidance, for two case studies. At first, we used the software to synthetically generate several thousands of conjunction events (below 5 km), by modifying the LEO population by adding five different megaconstellations (SpaceX Starlink, OneWeb, Amazon Kuiper, Guo Wang, and SatRevolution). Then, the effects of these megaconstellations on the generated conjunctions have been analyzed. It was pointed out how these new objects are going to not only increase the risk of having a collision but will also blow up the number of conjunction data messages. Furthermore, in a separate case study, we have also shown how different observations strategy (with different measurement accuracies) can have a significant impact on the quantities that are crucial for conjunction screening, such as the probability of collision and the miss distance. In summary, we can recap the main highlights of the work as follows:

- Kessler (in particular its probabilistic simulator module) can be used to generate conjunctions (and their associated CDMs) with different LEO populations and observations strategy, therefore allowing to experiment with various possible scenarios. This makes the tool not only useful for analyzing and predicting CDMs but also for being incorporated as a tool to design or approve future missions, constellations, and/or observation strategies. Furthermore, it can also be used to assess the current LEO environment and the key regions and objects in terms of collision risk;
- none of the tested megaconstellations seem to have a peculiar orbital geometry that would increase the collision risk of their close encounters with other resident space objects. Nonetheless, the increased number of close encounters due to the presence of megaconstellations causes the risk of having a collision in a given timeframe to considerably increase;
- once fully deployed, megaconstellations will massively increase the number of conjunction events below 5 km, with severe consequences both in terms of risk of collision and also the number of CDMs generated. It is estimated that Starlink would cause a $3.3\times$ increase, while OneWeb a $250\times$ increase, Amazon Kuiper a $1.6\times$ increase, Guo Wang a $2.2\times$, increase and SatRevolution a $1.35\times$ increase;
- we found that the number of conjunctions as a function of the distance at TCA can be represented using an empirical law (based on an exponential fitting function). With this, we find that by reducing the conjunction threshold at 1.2 km, the number of CDMs would be reduced by a factor of 10,000;
- we show how Kessler can also be used to find the most frequent objects that are encountered in conjunctions and to quantify their occurrences. In the analyzed cases, ASAT tests debris and collisions debris have been demonstrated to be the most frequent ones. This emphasizes the importance of avoiding

ASAT tests, as their generated cloud of debris poses a serious and lasting threat to space objects;

- we showed how large observation errors can cause the dilution of collision probability phenomenon, as well as a miscalculation of the miss distance;
- both experiments seem to suggest that improving the measurement errors of our sensor, through which we observe space objects, can be crucial in both performing more accurate conjunction analysis and avoiding over/under-estimation of collision risk, as well as massively reducing the number of CDMs, and therefore the burden on operators, by reducing the conjunction threshold.

ACKNOWLEDGMENTS

The authors would like to thank the UK Space Agency for the funding and continuous support during the development of the work. This was enabled by a UK Space Agency NSTP study, with reference UKSAG21_0073

REFERENCES

1. Giacomo Acciarini, Francesco Pinto, Sascha Metz, Sarah Boufelja, Sylvester Kaczmarek, Klaus Merz, José A Martinez-Heras, Francesca Letizia, Christopher Bridges, and Atılım Güneş Baydin. Spacecraft collision risk assessment with probabilistic programming. In *NeurIPS 2020: Machine Learning and the Physical Sciences Workshop*, 2020.
2. Giacomo Acciarini, Francesco Pinto, Francesca Letizia, José A Martinez-Heras, Klaus Merz, Christopher Bridges, and Atılım Güneş Baydin. Kessler: A machine learning library for spacecraft collision avoidance. In *8th European Conference on Space Debris*, pages 1–9, 2021.
3. S Aida and Kirschner M. Collision risk assessment and operational experiences for leo satellites at gsoc. In *Proceedings of the 22nd International Symposium on Space Flight Dynamics, Sao Jose dos Campos, Brazil*, 2011.
4. Salvatore Alfano. Relating position uncertainty to maximum conjunction probability. *The Journal of the Astronautical Sciences*, 53(2):193–205, 2005.
5. Vic Barnett. *Comparative statistical inference*, volume 522. John Wiley & Sons, 1999.
6. Atilim Güneş Baydin, Lei Shao, Wahid Bhimji, Lukas Heinrich, Lawrence Meadows, Jialin Liu, Andreas Munk, Saeid Naderiparizi, Bradley Gram-Hansen, Gilles Louppe, et al. Etalumis: Bringing probabilistic programming to scientific simulators at scale. In *Proceedings of the international conference for high performance computing, networking, storage and analysis*, pages 1–24, 2019.
7. Aaron C Boley and Michael Byers. Satellite mega-constellations create risks in low earth orbit, the atmosphere and on earth. *Scientific Reports*, 11(1):1–8, 2021.
8. Simon Burgis, Lukas Rohrmüller, Martin Michel, and Reinhold Bertrand. Simulation of satellites and constellations for the assessment of collision avoidance operations. *CEAS Space Journal*, pages 1–16, 2022.
9. Andrea Farkasvolgyi and Laszlo Csurgai-Horvath. Adverse effects of mega constellation systems on long-distance optical connections. In *2022 International Conference on Electrical, Computer, Communications and Mechatronics Engineering (ICECCME)*, pages 1–5. IEEE, 2022.
10. Babiker Fathelrahman, Michel Doyon, and Abbasi Viqar. The canadian space agency (csa) collision risk assessment and mitigation system (crams): Sharing the development and the operational challenges. *Quebec, Canada*, 2011.
11. T Flohrer, V Braun, H Krag, K Merz, S Lemmens, B Bastida Virgili, and Q Funke. Operational collision avoidance at esoc. In *Deutscher Luft-und Raumfahrtkongress, Rostok, Germany*, 2015.
12. James Lee Foster and Herbert S Estes. *A parametric analysis of orbital debris collision probability and maneuver rate for space vehicles*. NASA, National Aeronautics and Space Administration, Lyndon B. Johnson Space . . . , 1992.
13. Olivier R Hainaut and Andrew P Williams. Impact of satellite constellations on astronomical observations with eso telescopes in the visible and infrared domains. *Astronomy & Astrophysics*, 636:A121, 2020.
14. Ryan Hiles, Amos Alexander, Nicholas Herzer, Diana McKissock, Aaron Mitchell, and Jonathan Sapinoso. Report on 2020 mega-constellation deployments and impacts to space domain awareness. In *Proceedings AMOS Conference*, 2021.
15. Chikako Hirose, Yoshitaka Taromaru, Masaya Kameyama, Sadao Aoki, and Syuzo Isobe. Overview of jaxa space debris surveillance operations. In *SpaceOps 2006 Conference*, page 5817, 2006.
16. Donald J Kessler and Burton G Cour-Palais. Collision frequency of artificial satellites: The creation of a debris belt. *Journal of Geophysical Research: Space Physics*, 83(A6):2637–2646, 1978.
17. Frederic Joshua Krage. Nasa spacecraft conjunction assessment and collision avoidance best practices handbook. Technical report, 2020.
18. Nobuo Kudo, Chikako Hirose, and Ikumi Matsuda. The jaxa conjunction assessment process. In *SpaceOps 2010 Conference Delivering on the Dream Hosted by NASA Marshall Space Flight Center and Organized by AIAA*, 2010.
19. Robert Massey, Sara Lucatello, and Piero Benvenuti. The challenge of satellite megaconstellations. *Nature astronomy*, 4(11):1022–1023, 2020.

20. Jonathan C McDowell. The low earth orbit satellite population and impacts of the spacex starlink constellation. *The Astrophysical Journal Letters*, 892(2): L36, 2020.

21. K Merz, B Bastida Virgili, V Braun, T Flohrer, Q Funke, H Krag, S Lemmens, and J Siminski. Current collision avoidance service by esa's space debris office. In *Proceedings 7th European Conference on Space Debris, Darmstadt, Germany*, pages 18–21, 2017.

22. Theodore J Muelhaupt, Marlon E Sorge, Jamie Morin, and Robert S Wilson. Space traffic management in the new space era. *Journal of Space Safety Engineering*, 6(2):80–87, 2019.

23. Lauri Kraft Newman. The nasa robotic conjunction assessment process: overview and operational experiences. *Acta Astronautica*, 66(7-8):1253–1261, 2010.

24. Lorenzo Olivieri and Alessandro Francesconi. Large constellations assessment and optimization in leo space debris environment. *Advances in Space Research*, 65(1):351–363, 2020.

25. Francesco Pinto, Giacomo Acciarini, Sascha Metz, Sarah Boufelja, Sylvester Kaczmarek, Klaus Merz, José A Martinez-Heras, Francesca Letizia, Christopher Bridges, and Atılım Güneş Baydin. Towards automated satellite conjunction management with bayesian deep learning. In *NeurIPS 2020: AI for Earth Sciences Workshop*, 2020.

26. Jonas Radtke, Christopher Kebschull, and Enrico Stoll. Interactions of the space debris environment with mega constellations—using the example of the oneweb constellation. *Acta Astronautica*, 131:55–68, 2017.

27. A Rossi, L Anselmo, C Pardini, P Farinella, and A Cordelli. Interaction of the satellite constellations with the low earth orbit debris environment. In *Mission Design & Implementation of Satellite Constellations*, pages 327–335. Springer, 1998.

28. A Rossi, GB Valsecchi, and P Farinella. Collision risk for high inclination satellite constellations. *Planetary and Space Science*, 48(4):319–330, 2000.

29. Fabian Schiemenz, Jens Utzmann, and Hakan Kayal. Survey of the operational state of the art in conjunction analysis. *CEAS Space Journal*, 11(3):255–268, 2019.

30. Enrico Stoll, Klaus Merz, Holger Krag, Brian D'Souza, and Benjamin Bastida Virgili. Collision probability assessment for the rapideye satellite constellation. In *6th European Conference on Space Debris, Germany*, volume 22, page 25, 2013.

31. Haicheng Tao, Qinyu Zhu, Xueke Che, Xinhong Li, Wanxin Man, Zhibin Zhang, and Guohui Zhang. Impact of mega constellations on geospace safety. *Aerospace*, 9(8):402, 2022.

32. B Bastida Virgili, JC Dolado, HG Lewis, J Radtke, H Krag, B Revelin, C Cazaux, CAMILLA Colombo, R Crowther, and M Metz. Risk to space sustainability from large constellations of satellites. *Acta Astronautica*, 126:154–162, 2016.

33. Samuel S Wilks. Certain generalizations in the analysis of variance. *Biometrika*, pages 471–494, 1932.

34. Frank Wood, Jan Willem Meent, and Vikash Mansinghka. A new approach to probabilistic programming inference. In *Artificial intelligence and statistics*, pages 1024–1032. PMLR, 2014.

35. Yan Zhang, Bin Li, Hongkang Liu, and Jizhang Sang. An analysis of close approaches and probability of collisions between leo resident space objects and mega constellations. *Geo-spatial Information Science*, 25(1):104–120, 2022.